OPTIMIZING THE NSLS-IIU ENERGY FOR MAXIMUM BRIGHTNESS AT OPERATIONAL BEAM INTENSITY

V. Smaluk*, Brookhaven National Laboratory, Upton, United States

Abstract

The most updated complex bend achromat lattice for the high-brightness upgrade of NSLSII provides a record-low electron beam emittance of 23 pm at 3 GeV. However, collective effects of beam dynamics, especially intra-beam scattering, are the main limiting factors of emittance and brightness at operational beam Intensity. Since the emittance and collective effects are strongly dependent on the beam energy, we estimated the lowest possible emittance scaled with energy and intensity, taking into account intrabeam scattering, vacuum chamber impedance, and bunch lengthening by higher-harmonic RF cavities.

INTRODUCTION

The high-brightness upgrade of NSLS-II is one of the top priorities of Brookhaven National Laboratory. Since reducing the electron beam emittance is an efficient way to increase the brightness, the low-emittance lattice based on the complex bend approach is being developed for the NSLS-II upgrade (NSLS-IIU) [1]. However, a common feature of low-emittance synchrotrons is short and intense electron bunches. The high particle density leads to strong collective effects that significantly increase the emittance with the beam current.

So, the relevant machine design problem is not simply to minimize the natural emittance determined by the lattice only but to find optimal beam parameters for maximum brightness at operational beam intensity [2,3]. To solve this problem for NSLS-IIU, we use the following approach: 1) learn from the experience of other low-emittance rings; 2) set up a reliable technique to estimate emittance at operational intensities, including collective effects; 3) scale the operational emittance with energy, intensity, and lattice-determined emittance; 4) optimize the lattice design to achieve the minimum operational emittance.

BEAM INTENSITY LIMITATIONS

The most direct limit of the beam energy E and current I_b in a storage ring results from the synchrotron radiation power rapidly increasing with the beam energy:

$$P_{\rm rad} = I_b U_0 = I_b \frac{C_\gamma}{2\pi} E^4 \int \frac{1}{\rho^2} ds \, , \qquad (1)$$

where $C_\gamma = 8.846 \cdot 10^{-5}$ m/GeV^3, U_0 is the radiation energy loss per turn, ρ is the bending radius. This strong E^4 dependence explains why higher-energy light sources are generally operated at lower current; there are no light sources with the beam current exceeding 500 mA. Fig. 1 shows the operational beam current as a function of energy for several synchrotrons; all the data were found in published materials. The dashed line represents an empirical rule $I_b(E)$.

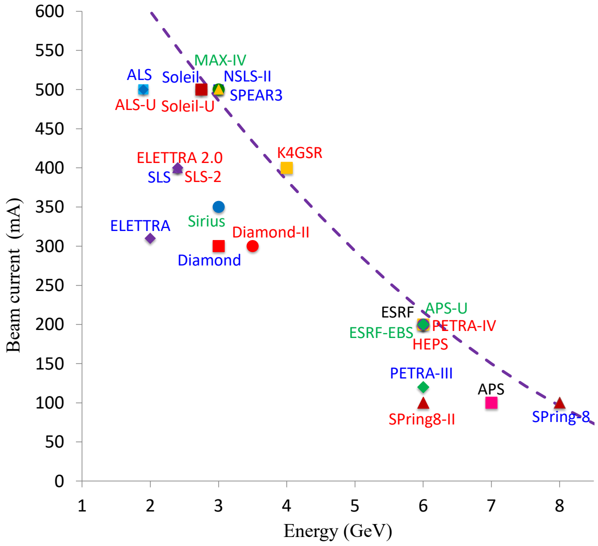

Figure 1: Operational beam current as a function of energy.

Vacuum-chamber heating provides a second practical constraint. The beam-induced power resulting from the interaction with resistive-wall impedance scales with the square of the beam current and increases when the chamber aperture is reduced.

$$P_{\rm rw} = \frac{k_{||} I_\Sigma^2}{N_b f_0} \, , \qquad (2)$$

where I_Σ is the average beam current, N_b is the number of bunches, f_0 is the revolution frequency, and $k_{||}$ is the longitudinal loss factor. That point matters particularly for low-emittance rings, including NSLS-IIU, where strong quadrupole magnets and advanced insertion devices require small-aperture chambers. The same small apertures also raise the impedance, which can drive collective instabilities.

INTRABEAM SCATTERING

Small-angle intrabeam scattering (IBS) results in an intensity-dependent 3D emittance growth. Although it does not lead to loss of particles, the emittance growth is significant in low-emittance rings, and this is a common problem for modern synchrotron light sources. Several IBS theories were developed: Piwinski theory for proton beams (two-particle collision kinematics, Rutherford cross-section) [4]; completely integrated modified Piwinski approximation (high energy beams) [5]; Bjorken&Mtingwa general solution (Gaussian bunch, variation of lattice parameters along the ring, no coupling) [6]; Bane's high-energy approximation with average lattice parameters [7]. We cross-checked

---

[*] smaluk@bnl.gov

these theories for the NSLS-IIU lattice [1] and found all the equations consistent within about 20%. However, the open question is if those theories based on the binary collision approach and Gaussian particle distributions are valid for the ultra-low emittance regime and essentially non-Gaussian longitudinal beam profile caused by higher-harmonic RF cavities (HHCs) [8]. Since the IBS growth rates are proportional to the particle density, we estimated it for several 3rd- and 4th-generation synchrotron light sources assuming the following conditions: no insertion devices ("bare" lattice), no higher-harmonic cavities (natural bunch length), design beam intensity, design zero-intensity emittance. The result is shown in Fig. 2. As one can see, particle density in the 4th-generation synchrotrons is two orders of magnitude higher than in previous machines, resulting in much stronger IBS effects.

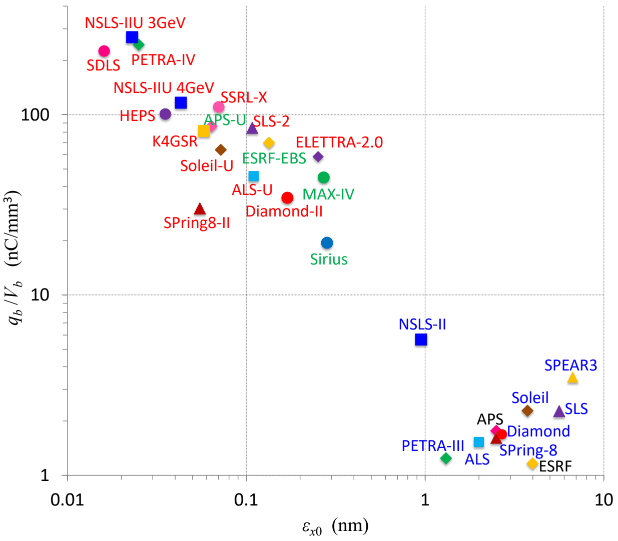

Figure 2: Charge density vs electron beam emittance.

OPTIMAL ENERGY FOR NSLS-IIU

The IBS strongly depends on the following beam parameters: energy, single-bunch current, longitudinal and transverse beam size. In synchrotron light sources, the emittance, energy spread, and bunch length at zero intensity are significantly affected by light-generating insertion devices (IDs), so we have to take IDs into account in calculations of collective effects. We included all present NSLS-II IDs and future high-performance undulators into the NSLS-IIU lattice model.

We calculated the combined effect of IBS, HHCs, and impedance. Following Bane's high-energy approximation for IBS [7], the longitudinal T_p^{-1}, horizontal T_x^{-1}, and vertical T_y^{-1} growth rates are

$$\frac{1}{T_p} \simeq \frac{r_0^2 cN}{32\gamma^3 \varepsilon_x \varepsilon_y \sigma_z \sigma_\delta^2}\left(\frac{\varepsilon_x\varepsilon_y}{\langle\beta_x\rangle\langle\beta_y\rangle}\right)^{1/4} \ln\frac{\langle\sigma_y\rangle\gamma^2\varepsilon_x}{r_0\langle\beta_x\rangle}, \tag{3}$$

$$\frac{1}{T_{x,y}} \simeq \frac{\sigma_\delta^2\left\langle\mathcal{H}_{x,y}\right\rangle}{\varepsilon_{x,y}}\frac{1}{T_p}, \tag{4}$$

$N = \frac{I_b}{ef_0}$ is the number of electrons per bunch; f_0 is the revolution frequency; r_0 is classical electron radius, $\mathcal{H}_{x,y} = \beta_{x,y}\eta_{x,y}'^2 + 2\alpha_{x,y}\eta_{x,y}\eta_{x,y}' + \gamma_{x,y}\eta_{x,y}^2$ is a function determined by the lattice. If the zero-current vertical emittance is caused by coupling κ only (no vertical dispersion, $\mathcal{H}_y = 0$), then T_y is ignored and $\varepsilon_y = \kappa\varepsilon_x$. We used the modified Zotter equation [9, 10] for the bunch lengthening caused by the beam interaction with longitudinal impedance:

$$\left(\frac{\sigma_t}{\sigma_{t0}}\right)^3 - \frac{\sigma_t}{\sigma_{t0}} = \frac{I_b\,\alpha_c}{4\sqrt{\pi}\,\nu_s^2\,\omega_0^3\sigma_{t0}^3\,E/e}\,\mathrm{Im}\left(\frac{Z_\parallel}{n}\right)_{\mathrm{eff}}, \tag{5}$$

where $\nu_s = \omega_s/\omega_0$ is the synchrotron tune; $\sigma_t = \sigma_z/c$; σ_{t0} is the bunch length at zero intensity. A typical effective normalized longitudinal impedance $\mathrm{Im}\left(Z_\parallel/n\right)_{\mathrm{eff}} = 0.5\ \Omega$ was assumed. We limit the beam-impedance interaction by the simplified model (5) in the absence of a detailed frequency-dependent impedance at the present stage of the machine design.

The RF voltage was scaled with the energy to keep the RF acceptance constant. The bunch lengthening provided by HHCs was implemented as a multiplication factor applied to the zero-current bunch length. An example of the NSLS-IIU beam emittance scaled with the beam current and energy is presented in Fig. 3. This graph corresponds to the betatron coupling $\varepsilon_y/\varepsilon_x = 0.35$ selected to provide the diffraction-limited vertical emittance of 8 pm at 3 GeV, the normalized longitudinal impedance of $Z_\parallel/n = 0.5\Omega$, and a moderate HHC bunch lengthening factor of 3. The red curve represents the empirical beam current limit shown in Fig. 1.

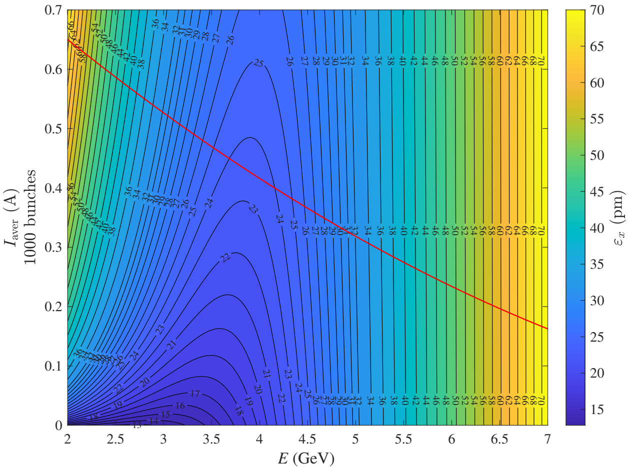

Figure 3: Combined effect of IBS, impedance, and higher-harmonic cavities on the beam emittance.

As one can see, there is an optimal energy to achieve the minimum emittance at operational beam intensity. For this NSLS-IIU lattice with IDs, the optimum is close to 4 GeV, determined by the zero-intensity emittance increase proportional to E^2 and IBS-driven emittance growth with intensity, approximately proportional to $1/E^3$. The longitudinal impedance increases the bunch length with intensity, helping to mitigate IBS, but not much. The key factor to mitigate IBS is the bunch lengthening provided by HHCs.

EFFECT OF HIGHER-HARMONIC CAVITIES ON THE OPTIMAL ENERGY

We explored the effect of bunch lengthening driven by higher-harmonic RF cavities on the optimal energy by scanning the energy along the empirical current limit for three cases: 1) no HHC, zero-current bunch length is determined by the lattice; 2) single HHC: $\sigma_{z0} \rightarrow \sigma_{z0} \times 3$; 3) sultiharmonic RF system: $\sigma_{z0} \rightarrow \sigma_{z0} \times 6$. The calculations were done for the same conditions: NSLS-IIU lattice with IDs, $\varepsilon_y/\varepsilon_x = 0.35$, $Z_{\|}/n = 0.5\Omega$, the result is presented in Fig. 4. More efficient bunch lengthening moves the optimal energy down. The positive effect of the bunch lengthening decreases with the energy.

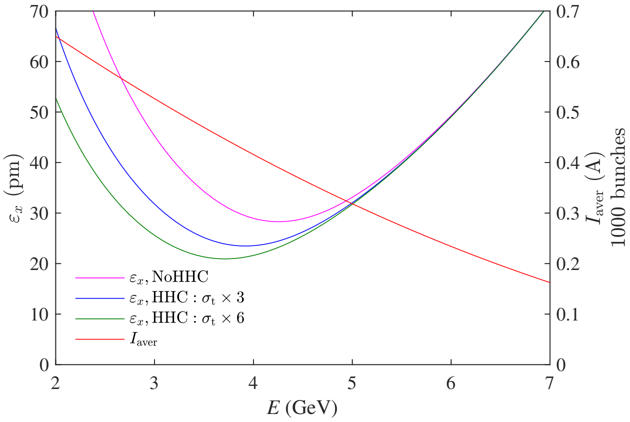

Figure 4: Effect of HHCs on the IBS-driven emittance growth.

SCALING WITH THE LATTICE-DETERMINED EMITTANCE

To check if the lattice design provides the optimal zero-intensity emittance, we explore the operational emittance dependence on the lattice-determined emittance. Since the IBS growth rates depend on both horizontal and vertical emittances, which, in turn, are affected by the IBS, we applied iterative solutions to find an equilibrium for a certain beam current. Accurate scaling of the lattice-determined emittance requires rematching of the lattice for each emittance point. To simplify the process, we scan the natural emittance ε_{x0} around the nominal value assuming average beta functions $\langle\beta_x\rangle \approx const$, $\langle\beta_y\rangle \approx const$ and use the coupling to set ε_x and ε_y. This approximation is valid for a rough estimate because the horizontal beta function is low in the complex bend magnets, mainly determining the emittance. Fig. 5 shows the results. With the present lattice design, we achieved a reasonably low natural emittance, limited by the maximum gradients in complex bends.

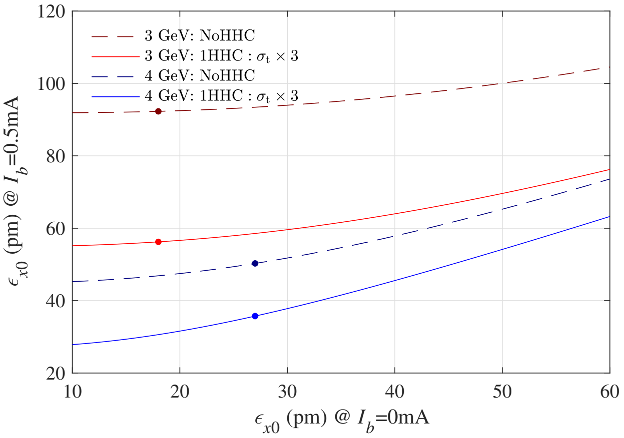

Figure 5: Effect of the zero-current emittance on the IBS-driven emittance growth.

CONCLUSION

Beam intensity in synchrotron light sources is mainly limited by RF power and beam-induced heating. Particle density in the 4th-generation synchrotrons is two orders of magnitude higher than in previous machines. Intrabeam scattering is the major effect limiting the beam emittance. A cross-check of the IBS equations showed that they are consistent to within about 20% for the NSLS-IIU complex-bend lattice. We used the high-energy approximation for fast emittance scaling with the energy and intensity. The open question is whether the theory is valid in the ultra-low-emittance regime and for an essentially non-Gaussian beam resulting from the bunch lengthening by higher-harmonic RF cavities. For a specific lattice, there is an optimal energy providing minimum emittance at the operational beam intensity. Bunch lengthening by higher-harmonic RF cavities is essential to provide low emittance at the operational beam intensity. More efficient bunch lengthening moves the optimal energy down. The positive effect of bunch lengthening decreases with the beam energy. With the present NSLS-IIU lattice design, we achieved a reasonably low natural emittance, limited by the maximum gradients in complex bends.

REFERENCES

[1] M. Song and T. Shaftan, "Design study of a low emittance complex bend achromat lattice", *Phys. Rev. Accel. Beams*, vol. 27, p. 061601, 2024. `doi:10.1103/PhysRevAccelBeams.27.061601`

[2] V. Smaluk and T. Shaftan, "Electron beam emittance at operational intensity in fourth-generation synchrotron light sources," *arXiv:2402.05204v2 [physics.acc-ph]*, 2024. `doi:10.48550/arXiv.2402.05204`

[3] V. Smaluk, T. Shaftan, and D. Hidas, "Ultimate brightness of a medium-energy synchrotron light source at operational beam intensity," *J. Synchrotron Radiat.*, vol. 32, no. 3, pp. 595–604, 2025. `doi:10.1107/S1600577525002723`

[4] A. Piwinski, "Intra-beam Scattering", in *Proc. 9th Int. Conf. on High Energy Accelerators (HEACC'74)*, Stanford, CA, USA, May 1974, pp. 405–409.

[5] K. Kubo, S.K. Mtingwa, and A. Wolski, “Intrabeam scattering formulas for high energy beams,” *Phys. Rev. Spec. Top. Accel. Beams* vol. 8, p. 081001, 2005. doi:10.1103/PhysRevSTAB.8.081001

[6] J.D. Bjorken and S.K. Mtingwa, “Intrabeam Scattering,” *Particle Accelerators*, vol. 13, pp. 115–143, 1983, https://s3.cern.ch/inspire-prod-files-a/a7d86ec1529ba6512d446523cd88c2d5

[7] K. Bane, H. Hayano, K. Kubo, T. Naito, T. Okugi, and J. Urakawa, “Intrabeam scattering analysis of ATF beam measurements”, SLAC National Accelerator Laboratory, Menlo Park, CA, USA, Rep. SLAC-PUB-8875, 2001.

[8] A. Khan, G. Stupakov, V. Smaluk, and T. Shaftan, “Limitations of the IBS theories with high-density beams”, presented at the 17th Int. Conf. on Part. Accel. (IPAC’26), Deauville, France, paper TUP2302, this conference.

[9] B. Zotter, “Potential-well bunch lengthening”, CERN, Geneva, Switzerland, CERN SPS/81-14 (DI), 1981, https://cds.cern.ch/record/129783

[10] D. Zhou, G. Mitsuka, T. Ishibashi, and K. Ban, “Potential-well bunch lengthening in electron storage rings,” arXiv:2309.00808 [physics.acc-ph], 2023. doi:10.48550/arXiv.2309.00808